Review of Scientific Instruments

Spatially resolved single crystal x-ray spectropolarimetry of wire array z-pinch plasmas

Cite as: Rev. Sci. Instrum. **89**, 015106 (2018); https://doi.org/10.1063/1.5006051
Submitted: 21 September 2017 . Accepted: 22 December 2017 . Published Online: 16 January 2018

M. S. Wallace, S. Haque, P. Neill, N. R. Pereira, and R. Presura

COLLECTIONS

This paper was selected as an Editor's Pick

View Online Export Citation CrossMark

ARTICLES YOU MAY BE INTERESTED IN

Prototype of the novel CAMEA concept–A backend for neutron spectrometers
Review of Scientific Instruments **89**, 015105 (2018); https://doi.org/10.1063/1.5018233

Note: An innovative method for $^{12}C^{4+}$ suppression in $^{18}O^{6+}$ beam production in an electron cyclotron resonance ion source
Review of Scientific Instruments **89**, 016103 (2018); https://doi.org/10.1063/1.5000426

Accounting for Debye sheath expansion for proud Langmuir probes in magnetic confinement fusion plasmas
Review of Scientific Instruments **89**, 013505 (2018); https://doi.org/10.1063/1.4995353

© 2018 Author(s).

REVIEW OF SCIENTIFIC INSTRUMENTS **89**, 015106 (2018)

Spatially resolved single crystal x-ray spectropolarimetry of wire array z-pinch plasmas

M. S. Wallace,[1,a)] S. Haque,[1] P. Neill,[1] N. R. Pereira,[2] and R. Presura[1,3,b)]
[1]*Physics Department and Nevada Terawatt Facility, University of Nevada, Reno, Nevada 89557, USA*
[2]*Ecopulse, Inc., Springfield, Virginia 22152, USA*
[3]*Voss Scientific, Albuquerque, New Mexico 87108, USA*

(Received 21 September 2017; accepted 22 December 2017; published online 16 January 2018)

A recently developed single-crystal x-ray spectropolarimeter has been used to record paired sets of polarization-dependent and axially resolved x-ray spectra emitted by wire array z-pinches. In this measurement, two internal planes inside a suitable crystal diffract the x-rays into two perpendicular directions that are normal to each other, thereby separating incident x-rays into their linearly polarized components. This paper gives considerations for fielding the instrument on extended sources. Results from extended sources are difficult to interpret because generally the incident x-rays are not separated properly by the crystal. This difficulty is mitigated by using a series of collimating slits to select incident x-rays that propagate in a plane of symmetry between the polarization-splitting planes. The resulting instrument and some of the spatially resolved polarized x-ray spectra recorded for a 1-MA aluminum wire array z-pinch at the Nevada Terawatt Facility at the University of Nevada, Reno will be presented. *Published by AIP Publishing.* https://doi.org/10.1063/1.5006051

I. INTRODUCTION

Many plasmas, including those found in solar flares,[1,2] laser-produced plasmas,[3,4] vacuum spark discharges,[5] electron beam ion traps,[6–8] dense plasma focus,[9,10] and x-pinches,[11,12] have electron distributions that are not isotropic but have a preferred direction, leading to the partial polarization of the emitted x-rays. Plasma polarization spectroscopy, or spectropolarimetry, may then be a useful diagnostic to determine the extent of the anisotropy, and thereby add information about the plasma beyond the temperature and density usually inferred from x-ray spectra without considering polarization.

X-ray spectra are obtained by scattering x-rays from an ordered structure. For a crystalline material, the waves with a given wavelength interfere constructively when scattered specularly at a certain angle, according to Bragg's law. A Bragg angle $\theta_B = 45°$ represents perpendicular scattering, for which the radiation polarized in the scattering plane is suppressed, and is therefore perfectly polarizing.[13] It was realized recently[14] that internal planes in certain crystals can be used to scatter simultaneously both orthogonal components of an incident x-ray beam. These internal planes have the same $2d$-spacing, and each of them is oriented at a nominal Bragg angle of 45°. The crystal diffracts radiation into two orthogonal directions, to produce two orthogonal linearly polarized x-ray components. The use of a single crystal for polarization-splitting[14] mitigates the difficulties met when using multiple crystals,[5,10–12] or multiple exposures.[3] The geometry for polarization-splitting crystals has been discussed extensively.[14–17] These references provide the basis for building a single-crystal x-ray spectropolarimeter and suggest suitable atomic transitions near the necessary 45° Bragg angle for various planes in several crystals. Polarization-splitting geometry of the hexagonal quartz crystal has been used to record paired sets of copper K-α spectra.[15] More recently, the polarization-splitting properties of Y-cut quartz were confirmed using linearly polarized synchrotron radiation.[18]

When two Bragg reflections are involved, accurate measurement of the polarization degree requires detailed understanding of how the spectral lines are formed. This can be complicated for extended sources. It will be shown in Secs. III–IV that polarization analysis is tractable if the x-ray incidence direction is symmetric to the polarizing planes. In practice, this has been achieved, for small discrete regions of the source, by using a series of collimating slits that provide space resolution in a manner similar to the Soller slits.[19] Results reveal that the x-rays emitted from aluminum z-pinches can be partially polarized, with different degrees of polarization at different locations. To our knowledge, this is the first use of a single-crystal x-ray spectropolarimeter on highly variable, single-shot, extended, pulsed-power plasmas, and the first recording of spatially resolved x-ray spectra including the polarization.

II. SINGLE-CRYSTAL SPECTROPOLARIMETER DESIGN

A schematic of the single-crystal spectropolarimeter used in this paper is shown in Fig. 1. In this study, to analyze the x-ray emission from aluminum wire array z-pinches, the crystal selected for the spectropolarimeter was X-cut quartz, with the surface parallel to the $(11\bar{2}0)$ planes. Figure 1 outlines the orientation of the surface planes of the crystal with points S, C, S, and R. The incident x-rays are split according to their polarization by the $(10\bar{1}0)$ and $(01\bar{1}0)$ planes. One set of polarizing planes, suggested by the red dashed plane, with corners 1, C, 1,

a)Electronic mail: mattheww@nevada.unr.edu
b)Present address: National Security Technologies, LLC, New Mexico Operations Office, Albuquerque, NM 87123, USA.

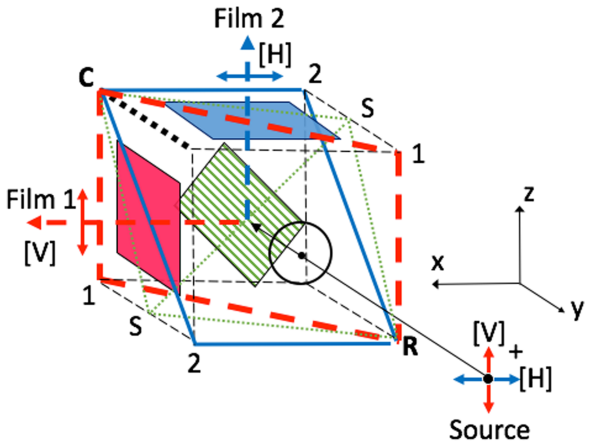

FIG. 1. Spectropolarimeter with a quartz crystal (green-striped rectangle) and two films: film 1 collects the vertical component of polarization, film 2 collects the horizontal component of polarization.

and R, scatters vertically polarized x-rays over 90° into $+\hat{x}$. Incident x-rays that are polarized horizontally, along $\hat{x}$, are suppressed and cannot scatter along $\hat{x}$. The other set of polarizing planes, suggested by the blue solid outlined plane, corners 2, C, 2, and R, scatters horizontally polarized x-rays into $+\hat{z}$. Both of the polarization-splitting planes lie 30° with respect to the surface.

The two polarization-splitting planes are only distinguished by a 60° rotation around the crystal symmetry axis and have the same $2d = 0.851$ nm. The corresponding energy for normal reflection ($\theta_B = 90°$) in the first order is $E_\perp = hc/2d = 1.457$ keV. The resulting energy for perpendicular scattering ($\theta_B = 45°$), $\sqrt{2}E_\perp$, is in the vicinity[14] of Al Ly-β and several He-like Al transitions. Transitions observed in the paper are listed in Table I. The relative reflection intensity for the two polarization components, away from 45°, is proportional to $\cos^2(2\theta_B)$ for ideal crystals, a condition met closely by flat quartz crystals.[14] Assuming that the crystal is ideal, over the range 42°–48°, the reflection intensity of the suppressed component is <1% of the desired component.

The rectangular crystal has the surface dimensions of 40 mm × 30 mm and a depth of 3 mm. The c-axis of the crystal's hexagonal structure is parallel to the longer (40 mm) edge. Figure 1 shows a schematic representation of the crystal mounted in its housing. The striped rectangle represents the crystal. The stripes represent the orientation of the c-axis, which is parallel to line CR. To correctly orient the polarization-splitting planes, the x-rays should have a nominal incidence angle ≅ 35.3° on the crystal surface. To achieve this, the crystal is mounted on a wedge[17] that has been precision machined. To optimize the signal-to-noise ratio, the crystal and mount are then positioned in a cubic brass housing of side length 100 mm. The crystal is positioned such that the center of the crystal face is located at the center of the housing. The housing has a 32 mm diameter hole located at the center of the front face, which facilitates mounting a variety of apertures and collimating assemblies. The solid rectangles on the top and left sides of the housing indicate the location of the x-ray film or image plates used to record polarization analyzed x-rays. They are positioned at the center of the cube sides, they are square, and have 50 mm side length.

TABLE I. X-rays from highly ionized Al with $h\nu \sim \sqrt{2}E_\perp = 2.061$ keV suitable for polarization by diffraction on quartz $(10\bar{1}0)$ planes.

Line	Transition	Energy (keV)	Bragg angle (deg)
He-γ	$1s^2$–1s4p	1.964	47.90
He-δ	$1s^2$–1s5p	2.008	46.52
He-ϵ	$1s^2$–1s6p	2.032	45.80
Ly-β	1s–3p	2.048	45.34

III. IMPORTANCE OF X-RAY INCIDENCE IN A PLANE SYMMETRIC TO THE POLARIZING PLANES

For the crystal used in this study, the polarizing planes are symmetric to the surface. For the polarized components to be diffracted at the same location of the crystal, the x-rays must be incident along the symmetry plane defined by the c-axis and the surface normal. When in this plane, the incident rays meet the polarization-splitting planes at the same Bragg condition, and the two reflections have the same exit angle. For a point source, rays can be constrained to a symmetry plane using a single slit, as shown in Fig. 2. In the figure, each ray path corresponds to different energy x-rays dispersed by the polarizing planes, with rays 1, 2, and 3 ranging from lowest to highest in energy. It should be noted that any plane perpendicular to the crystal surface and containing the c-axis is a valid symmetry plane. This property is exploited in Sec. IV to produce unambiguous polarized spectra from extended sources.

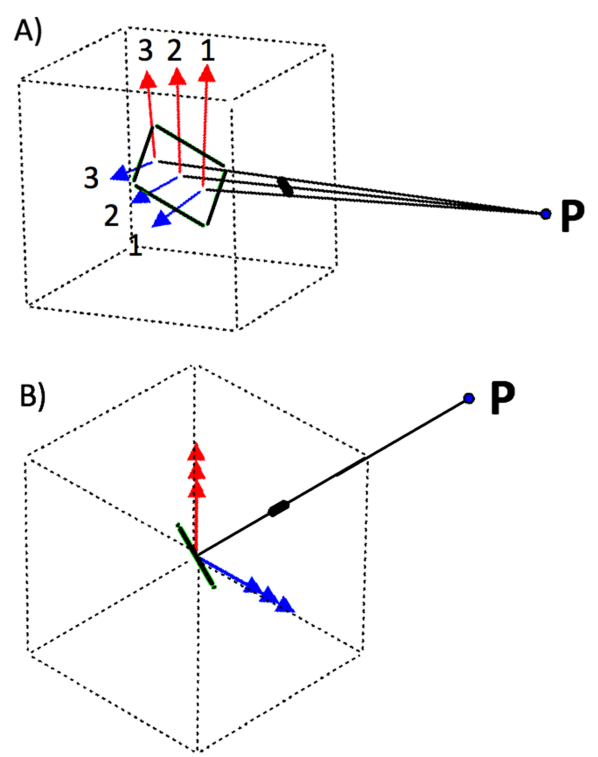

FIG. 2. Single-crystal spectropolarimeter using a slit to confine the x-rays from a point source to the symmetry plane. Polarization-splitting happens at the same energy for both polarizing planes: looking (a) from the side and (b) along the surface of the crystal with the line of sight parallel to the c-axis.

When the x-rays are not incident along a symmetry plane, the polarized components are diffracted from different regions of the crystal, and the corresponding spectral lines on the two detectors become difficult to correlate. This situation becomes particularly challenging for extended x-ray sources, typical for laboratory plasmas. For example, z-pinch plasmas often present a multitude of small sources of energetic x-rays, >1 keV, embedded in surrounding plasma that emits softer x-rays.[20] X-pinch wire-array configurations regularly produce single hot spots,[21,22] however, not in controllable fashion. Multiple sources make interpretation of spectropolarimetry difficult.[12] When two mutually orthogonal polarizing planes are used, multiple sources may create a space averaging effect for one plane and a source broadening or multiplet structure effect for the other plane. This has limited spectropolarimetry to single point-like sources in the past. The single-crystal spectropolarimeter with no restricting apertures exhibits the same problem.

In the case of multiple sources or an extended source, a single slit could be used with the single-crystal spectropolarimeter to provide spatial resolution. The top left of Fig. 3 depicts the spectropolarimeter fielded with a single slit for axial resolution of a typical z-pinch with multiple x-ray sources. The spectropolarimeter is oriented to monitor x-ray polarization components parallel (vertical) and perpendicular (horizontal) to the pinch axis. The slit and pinch are aligned so that rays from the center of the pinch axis are incident on the crystal along a plane of symmetry (see Fig. 2). Rays from the center of the pinch are incident on the crystal, and the films at locations represented by the solid black lines in Fig. 3.

Rays from other regions of the pinch do not propagate along symmetry planes. An example of this is shown in the figure with rays from a point near the cathode, the location that these rays hit the crystal, and the films are represented by black dotted lines. Rays from near the cathode do not propagate in a symmetry plane. They will intercept the polarization-splitting planes at different Bragg angles. When this happens, for a particular photon energy to access the correct Bragg angle, the two polarizing planes must utilize different ray paths. In this case, path length differences through the crystal can create signal attenuation differences that must be accounted for.

Discrepancies between the range of Bragg angles for the two polarization-splitting planes when considering regions that do not use a plane of symmetry shown in the plot in the top right of Fig. 3. In this plot, the vertical-axis represents a position along the pinch axis, and the horizontal-axis is the corresponding Bragg angle range for each location. The range for plane 1 (vertical component) is outlined with finely lined vertically striped red quadrilateral, and the range for plane 2 (horizontal component) is outlined with blue horizontally striped quadrilateral. For these calculations the anode-cathode gap is 20 mm, and the distance from the source to the slit is 120 mm. The bottom of Fig. 3 shows films recorded with a single slit in this configuration from an aluminum cylindrical wire array z-pinch. The recorded spectra demonstrate the importance of constraining x-rays to a plane of symmetry between the two polarization-splitting planes. In extreme cases, for any region of the pinch where the spectral drift between the two planes is large enough so that there is no spectral overlap between the two splitting planes spectral polarization analysis cannot be performed.

In conclusion, to facilitate meaningful single-crystal spectropolarimetric measurements, incident x-rays should be constrained to a plane of symmetry. For extended sources, this requires using arrays of collimating slits to confine the radiation to a symmetry plane for each region of the source. The construction of a multi-slit collimator and results obtained using it are discussed next.

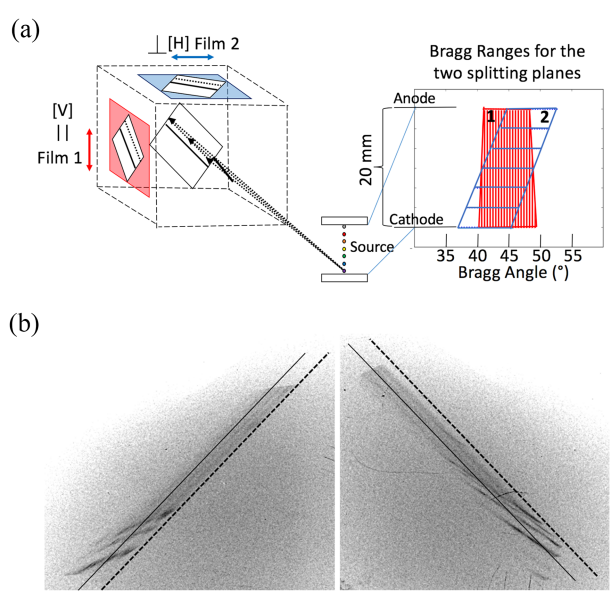

FIG. 3. Depiction of the single-crystal spectropolarimeter using a slit to analyze the spectrum of an extended source (top-left). The Bragg ranges for both polarization-splitting planes (top-right), using a single slit. A pair of spectropolarigrams from the Al cylindrical wire array z-pinch (bottom), recorded using a single slit.

IV. SINGLE-CRYSTAL SPECTROPOLARIMETRY OF EXTENDED SOURCES

A schematic of the spectropolarimeter with the collimating slit aperture is shown in Fig. 4. The aperture used here is made of 8 identical layers of 0.2 mm thick stainless steel sheets, each with a set of 11 slits and precisely aligned in a solid fixture. The spacing between the sheets has been arranged to prevent cross talk between neighboring slits, and each slit observes a

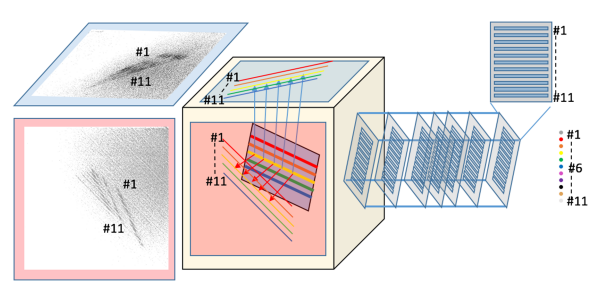

FIG. 4. Use of the multi-slit collimating aperture to enable the use of the single-crystal spectropolarimeter for extended sources.

different region along the 20 mm plasma column. This style of collimating slits is chosen over the conventional Soller slit[19] for ease of replacing a single front plate in the case of damage from debris during a shot. The projections of the slits on the crystal surface are oriented along the c-axis, confining rays narrowly around the symmetry plane for each opening. Each slit is 0.5 mm wide, and the centers of consecutive openings are separated by 1.3 mm. The total length, line-of-sight, of the collimator is approximately 70 mm. The distance from the front of the collimator to the pinch is 65 mm. In the current setup, each slit passes x-rays from a region ≅ 1.8 mm along the pinch axis, and thus the recorded spectropolarigrams are averaged over that region. Neighboring regions along the pinch axis are separated by ≅ 0.3 mm. Rays from different slits project at different heights sweeping diagonally on the film, and these projections are depicted in Fig. 4 as parallel solid lines in the film regions; the orientation of typical spectropolarigrams are shown with the cartoon of the setup.

Spectropolarimetry of an Al cylindrical wire array with eight 15 μm wires and 12 mm initial diameter was performed using the collimating aperture. The spectrum of the z-pinch was independently recorded with a KAP, potassium acid phthalate, crystal spectrometer. In addition to the spectrometer, a time-integrating pinhole camera was fielded to record the size and shape of the plasma column. Results from these diagnostics are shown in Fig. 5. The pinhole image outlines the regions observed with the collimating aperture. Region one corresponds to a region nearest the anode, and region eleven corresponds to a region nearest the cathode. Transitions which are observed by the spectropolarimeter are indicated in the spectrum within a dotted frame (see Table I). Spectropolarigrams for the same shot are shown in Fig. 6. They have been rotated so that the spectrum from every opening is oriented horizontally, and the corresponding regions are numbered.

The view of the spectropolarimeter in Fig. 7 shows that different regions of the plasma column are aligned differently to their respective slit. This alignment manifests itself with different spectral ranges, or energy ranges, covered for each region. The expected Bragg ranges covered for each region with the collimator are shown in the right of Fig. 7, assuming very narrow collimating slits.

Lineouts of the spectropolarigrams indicated in Fig. 6 by the solid arrows are shown in Fig. 8. For each slit, the

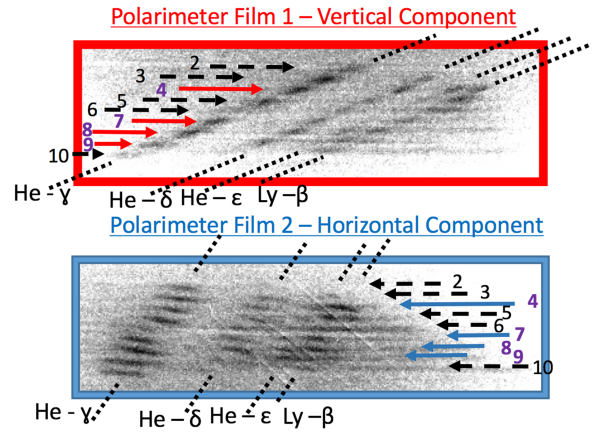

FIG. 6. Spectropolarigrams obtained using the multi-slit collimator. The numbered arrows indicate the individual slit collimators, and the continuous arrows point to the regions discussed in more detail in the text.

plot shows one lineout for each of the two polarizations. The vertical component is indicated by the dotted-red line and the horizontal component by the solid-blue line. Preliminary analysis of the raw data was performed after background subtraction and integration to determine the total intensity for each spectral line. It is assumed that if x-rays from the source are unpolarized there should be equal total intensity on the two films. Under this assumption, the nearly identical spectra recorded through slit 8 show no evidence of non-zero polarization. Under the same assumption, the spectra for slit 4, the He-δ, and He-γ lines appear to be polarized vertically, i.e., parallel to the pinch axis. For slit 4, at the higher energy side of the spectra, the Ly-β line is near the slit edge. This shows the appearance of partial horizontal polarization for this line. However, this result cannot be verified.

In the spectropolarigrams obtained though slit 7, all transitions from Table I are within the spectral range. In slit 7, for the Ly-β line it appears that the horizontal (blue) component is slightly stronger than the vertical (red) component. Although the difference for slit 7 are smaller than for slit 4, the He-δ and He-γ lines appear to have a vertical component that is slightly stronger than the horizontal component. In contrast, for slit 9, He-δ shows a vertical polarization, and the He-ϵ and Ly-β lines are not resolved. Diffraction of these two spectra from a single crystal rules out any line-of-sight differences, hence the

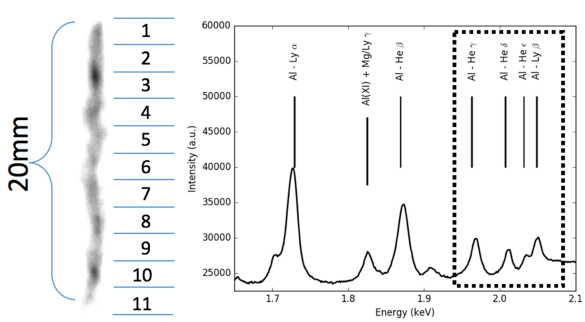

FIG. 5. (left) Pinhole image, regions 1 through 11 indicate the plasma region aligned to each slit of the collimator used with the spectropolarimeter. (right) Spatially averaged spectra from the KAP spectrometer. The 4 lines observed in the spectropolarimeter are indicated by the dotted frame.

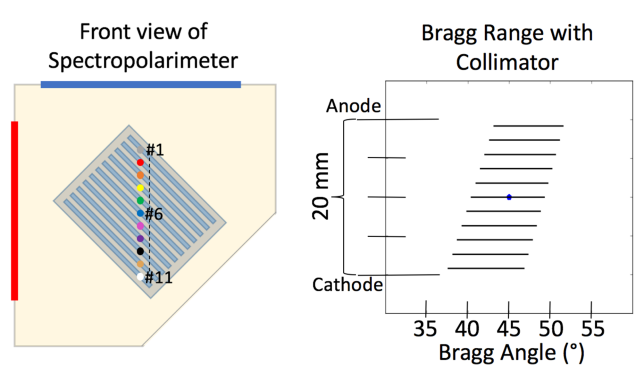

FIG. 7. (left) Front view of the spectropolarimeter and (right) the resulting spectral range for the two planes with the collimating aperture.

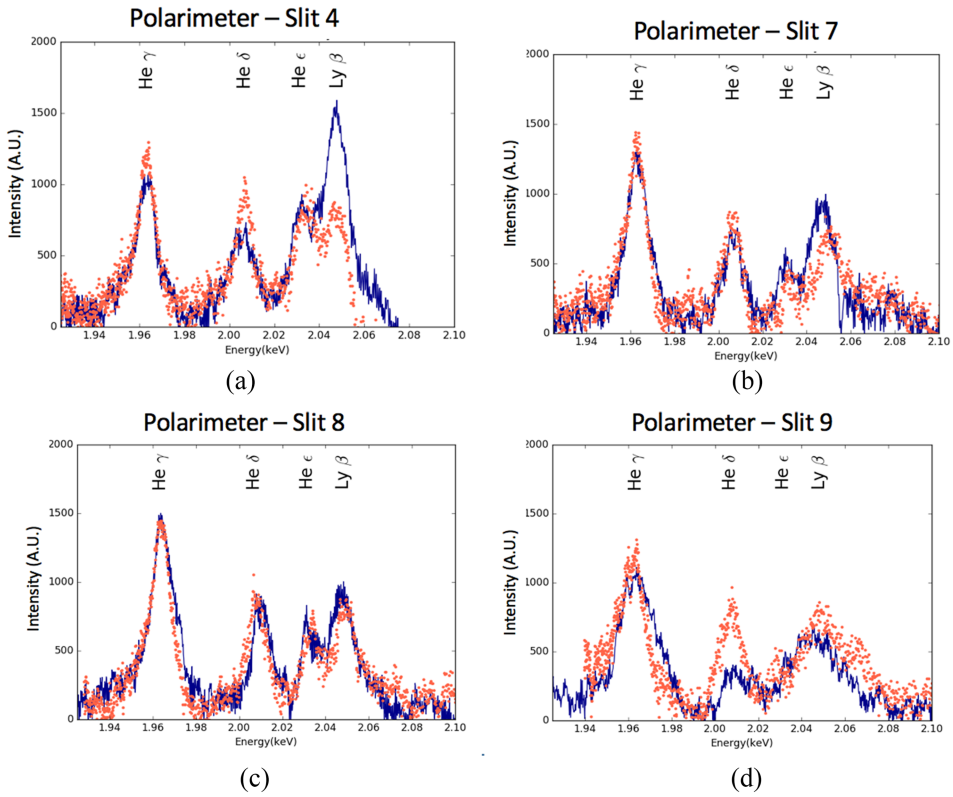

FIG. 8. Vertically (red-dotted lined) and horizontally (blue-solid lined) polarized spectra around 2 keV for four z-pinch regions selected by Slit 4, Slit 7, Slit 8, and Slit 9.

spectral difference should be interpreted as partial polarization whose degree varies along the z-pinch axis. This discussion of the results is qualitative; in the future, a more quantitative discussion is needed.

V. CONCLUSIONS

The use of a single-crystal x-ray spectropolarimeter to record simultaneously two spatially resolved sets of polarized spectra from Al wire array z-pinches has been demonstrated. For sources with spatial extent, as in the z-pinches here, the formation of the recorded spectrum is complicated. A detailed study of spectrum formation by reflections from these planes suggests the necessity to keep the x-rays confined to the symmetry plane of the polarization-splitting planes. This was achieved using a series of collimating slits, enabling spectropolarimetry of non-point sources. A future collimator design could have smaller slit openings to improve spatial resolution.

The spatially resolved spectropolarimetric measurements here suggest that different regions of the plasma can have different degrees of polarization for the transitions measured from H-like and He-like Al ions. This is the first use of a single-crystal x-ray spectropolarimeter on single-shot, extended x-ray sources such as z-pinches. In the future, a more quantitative analysis of the results is needed, supported with additional diagnostics.

ACKNOWLEDGMENTS

We would like to thank Dr. E. O. Baronova for supplying the crystals used in this work. We also would like to thank Nevada Terawatt Facility personnel A. Astanovitskiy, V. Nalajala, and O. Dmitriev for operations during Zebra shots. We would also like to thank Dr. T. Darling, A. Astanovitskiy, O. Dmitriev, and W. Cline for various components of the spectropolarimeter.

This work was supported by the U.S. Department of Energy, National Nuclear Security Administration Grant No. DE-NA0001834 and cooperative Agreement No. DE-FC52-06NA27616 to the University of Nevada at Reno.

[1] R. Novick, Space Sci. Rev. **18**, 389 (1975).
[2] M. Hart, Nucl. Instrum. Methods Phys. Res., Sect. A **316**, 416 (1992).
[3] J. C. Kieffer, J. P. Matte, H. Pépin, M. Chaker, Y. Beaudoin, T. W. Johnston, C. Y. Chien, S. Coe, G. Mourou, and J. Dubau, Phys. Rev. Lett. **68**, 480 (1992).
[4] Y. Inubushi, Y. Okano, H. Nishimura, T. Kai, T. Kawamura, S. Fujioka, D. Batani, A. Morace, R. Redaelli, C. Fourment, J. Santos, G. Malka, A. Boscheron, A. Casner, M. Koenig, T. Nakamura, T. Johzaki, H. Nagatomo, and K. Mima, J. Phys.: Conf. Ser. **112**, 022105 (2008).
[5] F. Walden, H. J. Kunze, A. Petoyan, A. Urnov, and J. Dubau, Phys. Rev. E **59**, 3562 (1999).
[6] P. Beiersdorfer, D. A. Vogel, K. J. Reed, V. Decaux, J. H. Scofield, K. Widmann, G. Hölzer, E. Förster, O. Wehrhan, D. W. Savin, and L. Schweikhard, Phys. Rev. A **53**, 3974 (1996).
[7] A. S. Shlyaptseva, R. C. Mancini, P. Neill, P. Beiersdorfer, J. R. Crespo López-Urrutia, and K. Widmann, Phys. Rev. A **57**, 888 (1998).
[8] P. Hakel, R. C. Mancini, C. Harris, P. Neill, P. Beiersdorfer, G. Csanak, and H. L. Zhang, Phys. Rev. A **76**, 012716 (2007).
[9] E. O. Baronova, G. V. Sholin, and L. Jakubowski, JETP Lett. **69**, 921 (1999).
[10] E. O. Baronova, G. V. Sholin, and L. Jakubowski, Plasma Phys. Controlled Fusion **45**, 1071 (2003).
[11] A. S. Shlyaptseva, S. B. Hansen, V. L. Kantsyrev, B. S. Bauer, D. A. Fedin, N. Ouart, S. A. Kazantsev, A. G. Petrashen, and U. I. Safronova, Rev. Sci. Instrum. **71**, 1241 (2001).
[12] E. O. Baronova, J. Larour, F. B. Rosmej, and F. Y. Khattak, J. Phys.: Conf. Ser. **653**, 012145 (2015).

[13]E. Wagner and P. Ott, Ann. Phys. **84**, 425 (1928).
[14]E. O. Baronova and M. M. Stepanenko, Plasma Phys. Controlled Fusion **45**, 1113 (2003).
[15]E. O. Baronova, M. M. Stepanenko, and A. M. Stepanenko, Rev. Sci. Instrum. **79**, 083105 (2008).
[16]N. R. Pereira, J. Mod. Opt. **5**, 2563 (2007).
[17]N. R. Pereira, High Energy Density Phys. **5**, 89 (2009).
[18]N. R. Pereira, R. Presura, M. Wallace, and A. Kastengren, Rev. Sci. Instrum. **85**, 073502 (2014).
[19]W. Soller, Phys. Rev. **24**, 158–167 (1924).
[20]N. R. Pereira and J. Davis, J. Appl. Phys. **64**(3), R1 (1988).
[21]D. H. Kalantar and D. A. Hammer, Rev. Sci. Instrum. **66**(1), 779 (1995).
[22]T. A. Shelkovenko, S. A. Pikuz, D. A. Hammer, Y. S. Dimant, and A. R. Mingaleev, Phys. Plasmas **6**(7), 2840 (1999).